Measurement of Quantal Secretion Induced by Ouabain and Its Correlation with Depletion of Synaptic Vesicles

C. HAIMANN, F. TORRI-TARELLI, R. FESCE, and B. CECCARELLI
Department of Medical Pharmacology, Consiglio Nazionale delle Richerche, Center of Cytopharmacology and Center for the Study of Peripheral Neuropathies and Neuromuscular Diseases, University of Milano, 20129 Milano, Italy.

ABSTRACT Ouabain (0.1 and 0.05 mM) was applied to frog cutaneous pectoris nerve-muscle preparations bathed in modified Ringer's solution containing either 1.8 mM Ca^{2+} (and 4 mM Mg^{2+}) or no added Ca^{2+} (4 mM Mg^{2+} and 1 mM EGTA). During the intense quantal release of acetylcholine (ACh) induced by ouabain, the parameters of the miniature endplate potentials (mepps) were deduced from the variance, skew, and power spectra of the endplate recordings by applying a recently described modification of classical fluctuation analysis. Often the high frequency of mepps is not stationary; therefore, the signal was high-pass filtered (time constant of the resistance-capacitance filter of 2 ms) to remove the errors introduced by nonstationarity. When ouabain was applied in the presence of Ca^{2+}, mepp frequency started to rise exponentially after a lag of 1.5–2 h, reached an average peak frequency of 1,300/s in ~30 min, and then suddenly subsided to low level (10/s). In Ca^{2+}-free solution, after a shorter lag (1–1.5 h), mepp frequency rose to peak rate of 700/s in ~20 min and then gradually subsided. In spite of the different time course of secretion in the two experimental conditions, the cumulative quantal release was not significantly different ($7.4 \pm 1.3 \times 10^5$ in Ca^{2+}-containing and $8.8 \pm 2.7 \times 10^5$ in Ca^{2+}-free solutions). 60 min after the peak secretion, the muscles were fixed for observation in the electron microscope. Morphometric analysis on micrographs of neuromuscular junctions revealed in both cases a profound depletion of synaptic vesicles and deep infoldings of presynaptic membrane. This rapid depletion and the lack of uptake of horseradish peroxidase suggest that ouabain impairs the recycling process that tends to conserve the vesicle population during intense secretion of neurotransmitter. The good correlation observed between the reduction in the store of synaptic vesicles and the total number of quanta of ACh secreted in the absence of a vigorous membrane recycling strongly supports the view that the secretion of a quantum of ACh requires the fusion of a synaptic vesicle with the axolemma.

The discovery of synaptic vesicles and the evidence for the quantal nature of transmitter release led to the hypothesis that transmitter is stored in and released from the vesicle by a process of exocytosis (15, 16). This hypothesis is accepted by many investigators but is challenged by others who suggest that the membrane of the nerve terminal contains channels that remain open for a relatively fixed period of time, allowing the diffusion of a fixed amount of cytoplasmic acetylcholine (ACh)[1] (for different points of view, see references 8 and 35). One of the major impediments to the general acceptance of the vesicle hypothesis is the difficulty in obtaining an adequate

[1] Abbreviations used in this paper: ACh, acetylcholine; BWSV, black widow spider venom; HRP, horseradish peroxidase; α-LTx, α-Latrotoxin; mepp, miniature endplate potential; RC, resistance-capacitance.

quantitative correlation between the number of vesicles present in the terminals at a given time and the total number of quanta of transmitter released. The number of synaptic vesicles present can be measured by morphometric analysis of electron micrographs, but the total number of quanta secreted is difficult to measure at rapidly secreting terminals. A new statistical method (33), based upon an extension (31) of Campbell's theorem (6), allows a reliable estimate of the amplitude and frequency of occurrence of miniature endplate potentials (mepps) under a variety of conditions where the rate of asynchronous release is high and the individual potentials so overlap that they cannot be counted. This method has been tested with computer-simulated data and applied to records obtained from neuromuscular junctions exposed to La^{3+} (33) and black widow spider venom (BWSV) (19).

We applied this modified procedure of fluctuation analysis to endplate records obtained in frog cutaneous pectoris muscle treated with ouabain (G-strophantin), a cardiac glycoside that causes a massive, transient, and Ca^{2+}-independent increase in the rate of secretion of quanta of neurotransmitter (1, 4). The total release of quanta of ACh induced by this cardiac glycoside was computed and correlated with the morphometric measurements of the changes in ultrastructure of the nerve terminals that occurred as a result of the secretory process. Some of the general features of the nerve terminal ultrastructure after treatment with digoxin or ouabain have been previously reported by others (3, 14).

At nerve terminals, during intense release of neurotransmitter, vesicle membrane cycles repeatedly between the axolemma and the axoplasm (11, 12, 22). Ouabain induces a rapid depletion of synaptic vesicles, which suggests an impairment of the endocytotic process. Therefore, we examined in the electron microscope the uptake of horseradish peroxidase (HRP) to obtain information about the size of the recovery limb of the recycling process under the effect of this cardiac glycoside.

Quantal release, nerve terminal ultrastructure, and uptake of HRP from muscles stimulated with ouabain in a solution with no added Ca^{2+} were compared with the same parameters obtained with a normal concentration of Ca^{2+} (1.8 mM), to test the previous suggestion that endocytosis of synaptic vesicles may be Ca^{2+}-dependent (9).

MATERIALS AND METHODS

Electrophysiology: Cutaneous pectoris nerve–muscle preparations were dissected out from frogs, *Rana pipiens*, of 2-in. body length (Connecticut Valley, Biological Supply Co., Southampton, MA) and mounted in a lucite chamber. The composition of the standard Ringer's solution was (in mM): Na^+, 116.2; K^+, 2.1; Ca^{2+}, 1.8; Cl^-, 116.9; HPO_4^{2-}, 2; $H_2PO_4^-$, 1; pH 6.9. To obtain Ca^{2+}-free solutions 1 mM of EGTA (Sigma Chemical Co., St. Louis, MO) was added to Ringer's solution containing no added Ca^{2+} and 4 mM Mg^{2+}. EGTA was dissolved in excess NaOH, titrated with HCl to pH 7.2, and diluted to make a concentrated stock solution isotonic with Ringer's solution. A stock solution of 10 mM ouabain (G-strophantin, Sigma Chemical Co.) was daily prepared and diluted with the bathing solution as required. The chamber was flushed several times with fresh solution whenever the composition of the bathing solution was changed and also during the prolonged incubation with ouabain. Paired muscles from individual frogs were used in all experiments in which the effects of Ca^{2+}-free and Ca^{2+}-containing solutions were compared. The same dose of ouabain was applied to the two muscles, one bathed in Ca^{2+}-free solution, the other in standard Ringer's solution modified by the addition of 4 mM Mg^{2+} (modified Ringer's solution). All experiments were run at room temperature.

Endplate regions were impaled with glass microelectrodes filled with 3 M KCl (resistance 20–30 Mohm), and the membrane potential recorded with a conventional high input impedance amplifier. The output of the amplifier was displayed on a dual beam oscilloscope (Tektronix S.p.A., Milano, Italy), both as a high gain AC coupled record (input time constant 0.33 or 1.0 s) for monitoring the mepps, and as a low gain DC record for monitoring the absolute value of the membrane potential. Both outputs were stored with a magnetic tape recorder (Racal 4DS, Racal Recorders, Ltd., Southampton, Hampshire, England) with 2,500-Hz bandwidth. A record ~10-min long was taken in the control solution to provide baseline values for the subsequent offline computation, and then the experimental solution was flushed in. When the mepp frequency began to increase, recording was resumed and maintained throughout the entire experiment. 1 h after the peak secretion induced by ouabain, the muscles were fixed and processed for electron microscopy. α-Latrotoxin (α-LTx), the active component of BWSV, was applied at the end of two experiments (see Results). The α-LTx was purified and the activity tested as previously described (20). Concentrated α-LTx was added directly to the bathing solution to give a final concentration of 2 μg/ml.

When not otherwise specified reagents have been supplied by Merck (Bracco S.p.A., Milano, Italy).

Determination of mepp Frequency and Amplitude by Fluctuation Analysis: The asynchronous quantal release of ACh, when stimulated by various agents, generates at neuromuscular junction random processes that can be studied by fluctuation analysis techniques.

The statistical properties of a fluctuating signal produced by the linear summation of elementary events occurring at random (shot noise) have been extensively studied (31). When the rate of the elementary events is stationary, the mean value of the shot noise is given by the mean frequency of the events, $\langle r \rangle$, times their amplitude, h, times the integral of their time course or waveform, $w(t)$:

$$\text{mean} = \langle r \rangle h \int_0^\infty w(t)\mathrm{d}t. \quad (1)$$

The variance (second central moment) of the signal is given by

$$\text{variance} = \langle r \rangle h^2 \int_0^\infty w^2(t)\mathrm{d}t. \quad (2)$$

The skew (third central moment), or average value of the cube of the deviation of the signal from its mean value, is given by

$$\text{skew} = \langle r \rangle h^3 \int_0^\infty w^3(t)\mathrm{d}t. \quad (3)$$

For the mepp at the endplate, Segal et al. (33) demonstrated that (*a*) the mepp waveform is well represented by the difference of two exponentials:

$$w(t) = \exp(-t/\theta_1) - \exp(-t/\theta_2).$$

This approximation holds well at least as far as the average of the integrals in Eqs. 1–3 over a population of mepps are concerned; (*b*) the decay time constant, θ_1, and the rise time constant, θ_2, of the mepp can be deduced either by curve fitting the waveform of the average of many individual mepps or from the power spectrum obtained from the fluctuating signal recorded at the endplate region; (*c*) known $w(t)$ mepp frequency, and amplitude are reliably measured from the variance and skew of endplate records, using Eqs. 2 and 3. This allows neglecting the mean signal, which is not reliable because sources of depolarization other than mepps may contribute to it. Better results are obtained if the signal is high-pass filtered, because this procedure removes the contributions to the moments due to slow changes in membrane potential or mepp frequency. mepp frequencies up to about 10 thousands per second are reliably measured with this procedure, with error in the order of 10%.

The computations of power spectra, variance, and skew of electrophysiological recordings were performed on a Digital Equipment Corp. (Maynard, MA) PDP 11/23 plus computer, after digitization at a sampling rate of 2.5 kHz. Groups of eight power spectra were computed at regular intervals during the experiment through fast Fourier transforms (Digital Equipment Corp. FFT routine) over the range 0.25–1,250 Hz; they were averaged and smoothed over frequency according to standard procedures (2, 33). Baseline power spectra were measured in Ringer's solution at the beginning of the experiments and subtracted from the data. When the mepps did not overlap, the time constants (θ_1 and θ_2) were determined by fitting the difference of two exponentials to the average of 20–30 isolated mepps. At high mepp frequencies, mepp waveform must be deduced from the power spectra. Most of the spectra obtained in ouabain (see Results) were not flat (white) at the low frequency end, as it would be expected for shot noise with event duration of a few milliseconds (32). The most likely source of these deviations are nonstationarity in mepp frequency

(e.g., bursting secretion) and membrane noise unrelated to mepps. Both phenomena would vitiate the results of fluctuation analysis. However, a nonstationary frequency, $r(t)$, adds to the variance extracomponents that are limited to the frequency bandwidth of $r(t)$ itself (31, 32), and its contributions to the skew are also additive and limited to the same bandwidth (16). A high-pass filter, which cuts off the section of the power spectrum containing extracomponents, will then remove their contribution to both the variance and the skew, whether the extracomponents are due to nonstationarity in mepp frequency or to membrane noise unrelated to mepps. The filtered record can then be analyzed by the same procedures applied to stationary records. This procedure has been tested by analyzing computer-simulated nonstationary endplate records (18) and applied to experimental endplate records obtained during the effect of BWSV (19).

The time constants of the mepps were deduced from the power spectra by fitting the product of two Lorentzians (the spectrum produced by the difference of two exponentials) to the data. The computer displayed the data, the analytical curve, and the difference between the two; the parameters of the Lorentzians were adjusted until the difference was minimum. In fitting the spectra, the deviations from white behavior at low frequency, discussed above, were neglected. Also neglected was the high frequency section where data points were less than twice the baseline.

mepp frequency and amplitude were determined, using the above Eqs. 2–3, from the variance and skew of the endplate records. Variance and skew were computed over 10-s sections of the records, filtered through a high-pass resistance-capacitance (RC) of 2 ms. The moments of three successive sections were averaged, and the corresponding moments of the baseline were subtracted.

Morphology: The muscles were fixed in the recording chamber with a cold solution of 2% OsO_4 (Polysciences, Inc., Warrington, PA) in 0.1 M phosphate buffer, pH 7.2, for 90 min at 4°C. Control muscles were soaked in similarly modified solutions without ouabain. Most of the experimental muscles were fixed ~1 h after the peak of release. Recovery was studied in six preparations: standard Ringer's fluid was applied 60 min after the mepp frequency had attained its peak value, and the muscles were fixed 2 h later. Small specimens, containing suspected endplate regions, were dissected out and block-stained with 0.5% uranyl acetate in Veronal buffer for 45 min. They were dehydrated and flat-embedded in EPON 812. Silver-gray sections were cut with a diamond knife (Diatome, Ltd., Bienne, Switzerland) on a Reichert-Jung Ultracut microtome (Reichert, Wien, Austria), double stained with uranyl acetate and lead citrate, and examined with an Hitachi H-600 electron microscope (Hitachi, Ltd., Tokyo, Japan). The correctness of the magnification given by the electron microscope was routinely checked with magnification standard grids (Balzers Union, Ltd., Liechtenstein). In some experiments the muscles were preincubated for 60 min, either in modified Ringer's or in Ca^{2+}-free solution, with 1.5% HRP (Sigma type II, 0.5%, and type VI, 1.0%) and 0.5% whale sperm myoglobin (Sigma type II). This incubation did not affect mepp frequency. Ouabain was then added to a final concentration of 0.05 mM, and the mepp frequency was monitored. When the mepp frequency reached its peak (see Results) the muscles were fixed for 60 min with 1% glutaraldehyde and 0.25% formaldehyde (freshly prepared from paraformaldehyde) in 0.1 M phosphate buffer. Small bits of tissue were treated to reveal sites of HRP activity (12, 21). They were then postfixed for 1 h with 2% OsO_4 in 0.1 M phosphate buffer (pH 7.2), dehydrated, and embedded as described above. Some sections from these preparations were observed unstained.

When not specified reagents for electron microscopy have been supplied by Fluka (Buchs, Switzerland).

Morphometric Analysis: Electron micrographs of longitudinally sectioned neuromuscular junctions from resting muscles and experimental muscles fixed 1 h after the peak of release induced by ouabain were examined. Equatorial sections of nerve terminal branches were printed at a final magnification of 42,000.

The following parameters were measured on each micrograph with the aid of a digiplan MOP-1 (Zeiss, Oberkochen, FRG): (*a*) area of the axoplasm comprised in the section; (*b*) length of axolemma; (*c*) length of axolemmal infoldings; (*d*) number of synaptic vesicles (diameter ~40 nm); (*e*) number of coated vesicles and coated pits; (*f*) total perimeter of large vesicular structures (diameter > 100 nm). The areas enclosed within the Schwann cell invaginations were subtracted from the area of nerve terminal cytoplasm, and the result was used to normalize all measurements. The Schwann cell invaginations were included with the axolemmal infoldings, both in control and in treated preparations. Synaptic vesicles were counted only when their membrane profile was clearly marked, and ghosts of vesicles were neglected.

In addition cross-sections of terminal branches printed at a final magnification of 30,000 were analyzed in control muscles, experimental muscles fixed 1 h after the peak of release induced by ouabain, and experimental muscles that had recovered for 2 h in Ringer's solution after the exposure to ouabain. The area of the axoplasm and the nerve terminal perimeter were measured in control terminals and in terminals that had recovered. Only areas of the axoplasm were measured in terminals that were fixed 1 h after the peak of release.

Mean and standard deviation were computed for each parameter; the statistical significance of all differences were determined by Student's *t* test.

RESULTS

Electrophysiology

The effect of ouabain on mepp frequency was studied on continuous intracellular recordings from single neuromuscular junctions. The concentrations used for quantitative analysis were 0.05 and 0.1 mM. Lower doses were used in preliminary experiments, but the data were not analyzed since the only obvious difference was a prolonged delay in the onset of the induced quantal secretion. The typical effect of ouabain in the presence of Ca^{2+} is shown in Fig. 1. After a long but variable delay the frequency of mepps increased, reached a peak in ~20 min, and then subsided to low values in ~40 min (see Table I). The onset of the effect (mepp frequency higher than 10/s) was 128 ± 13 min and 114 ± 31 min with 0.05 and 0.1 mM ouabain, respectively. A similar increase in the rate of secretion was observed in Ca^{2+}-free solution. The only obvious difference was a shorter latency: 84 ± 22 min in 0.05 mM, and 63 ± 9 min in 0.1 mM ouabain. In both experimental solutions a bursting pattern in mepp frequency was often observed.

These observations agree with the overall behavior previously reported for mammalian as well as frog neuromuscular junctions (1, 4, 17). The relatively rapid decline of mepp frequency from its peak value suggests that depletion of the quantal store occurs. In two experiments, 60 min after the peak of secretion induced by 0.1 mM ouabain, when the frequency had subsided to ~5/s, the preparations were perfused with Ringer's solution without ouabain for 90 min and then exposed to α-LTx (2 μg/ml) for 30 min. Before α-LTx was applied normal mepps at low frequency (~0.03/s) were still generated. An increase in mepp frequency would have been expected after α-LTx was applied if any recovery of quanta had occurred. α-LTx did not induce any changes in mepp frequency or time course. We therefore concluded that the terminals exposed to ouabain were exhausted of quanta of transmitter, and recovery had not occurred in spite of the extensive washing with fresh Ringer's solution.

mepp amplitude, time course, and frequency during the effect of ouabain were investigated in detail by applying the described fluctuation analysis procedure.

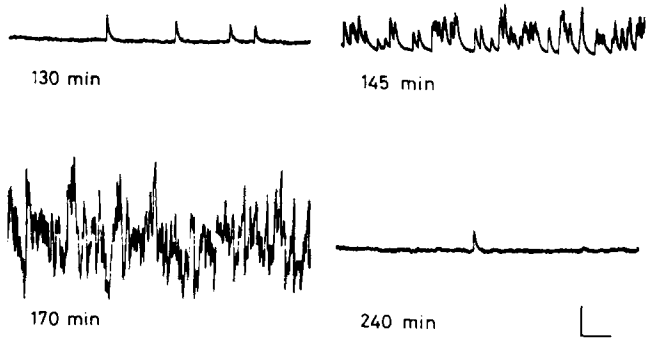

FIGURE 1 Intracellular recording of mepps obtained during the effect of ouabain 0.05 mM in modified Ringer's solution. The membrane potential was −87 mV at 130 and 145 min, −76 mV at 170 min, −88 mV at 240 min. Calibration bars: 1 mV, 100 ms.

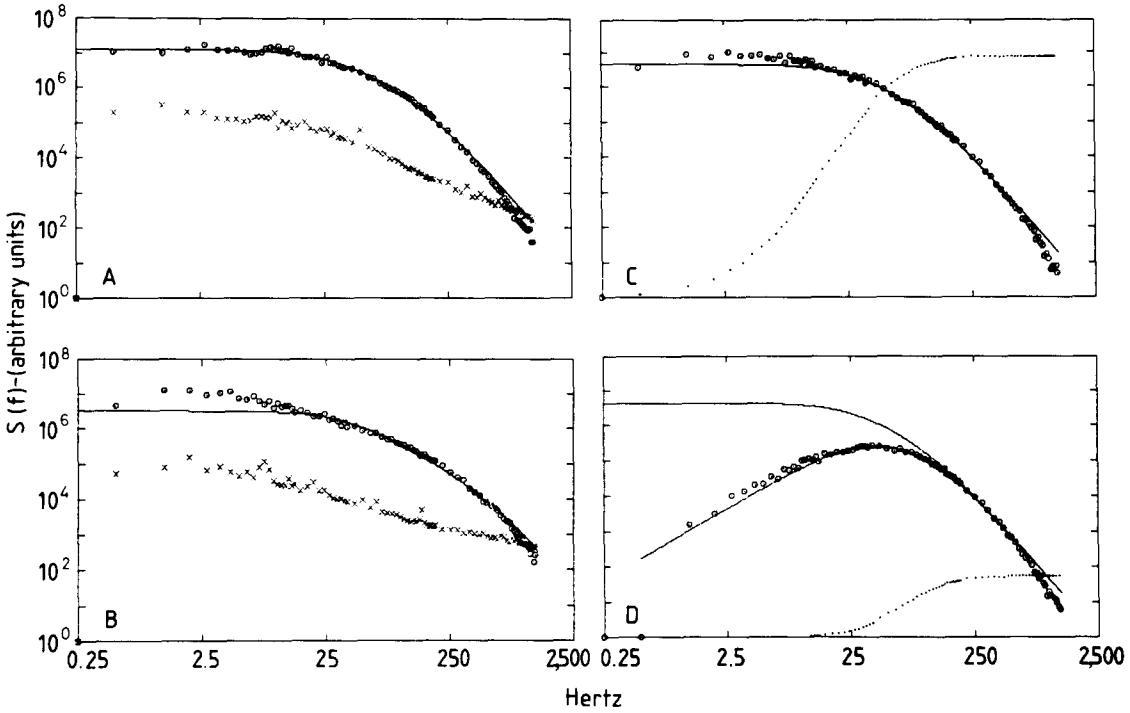

FIGURE 2 Power spectra of intracellular recordings at three rapidly secreting neuromuscular junctions. Ordinates: power per unit bandwidth, arbitrary units, logarithmic scale. Abscissae: frequency (Hz), logarithmic scale. (*A*) 0.05 mM ouabain in modified Ringer's solution. (*B*) 0.05 mM ouabain in Ca^{2+}-free Ringer's. (*C* and D) 0.1 mM ouabain in modified Ringer's solution, computed from the same record before and after filtering (RC = 2 ms). The experimental spectrum (O) in each panel is the average of eight spectra, further smoothed by frequency averaging. The baseline spectrum (lover curve in *A* and *B*: [x]) was subtracted before plotting. Solid lines are theoretical spectra for double exponentials fit to the data. The time constants of the double exponentials were: *A*, 5.38 and 0.84 ms; *B*, 4.39 and 0.28 ms; *C* and *D*, 6.05 and 1.27 ms. Note the very good fit of the data to the theoretical curve in *A*, and the good fit in *C* and *D* for frequencies higher than 20 Hz. The time constants obtained by fitting the theoretical curve to the data in *B* were not considered reliable because of the large distortion in the power spectrum, and thus the experiment was discarded. Dotted lines are the integrals of the spectra, on linear scale with arbitrary units, and the rightmost point represents the total power, i.e, the variance. The full scale value in *D* is half of that in C. The first data point falls below the curves in all spectra because the recording circuit was AC coupled (*A*, 1 s; *B* and *C*, 0.3 s).

Power Spectra of Active Endplate

The power spectrum of endplate recordings, which defines the frequency composition of the data, yields two basic pieces of information. (*a*) The spectrum should have the general shape expected from the waveform of the mepp, well approximated by the difference of two exponentials (33); if not, either mepp frequency is not stationary or other phenomena contribute to the signal. (*b*) The time constants deduced from the power spectrum define the waveform of the mepp; knowing this, mepp frequency and amplitude can be determined from the variance and skew of the signal.

Fig. 2 shows three examples of power spectra obtained from treated junctions during massive quantal release. The theoretical curves (solid lines) fit the whole spectra well only in four experiments out of thirteen (Fig. 2*A*). In these four experiments ouabain was applied in a Ca^{2+}-containing solution. In the remaining experiments, the points at low frequency (<10 Hz) fall above the theoretical curve (Fig. 2, *B* and *C*). Apart from possible changes in mepp waveform, spectral distortions might be due to factors such as nonstationary pattern of release or instability of the membrane potential. The variance and skew of the signal obtained in these conditions can give large errors in the estimate of mepp amplitude and frequency. It has been shown, both theoretically and experimentally, that these errors can be virtually removed by high-pass filtering the signal (18, 19). Fig. 2 *D* shows the effect of high-pass filtering the record of Fig. 2 *C*. The spectral points that deviate from the analytical shape do not contribute to the variance any more. This is shown by the total power plot in Fig. 2*D*, which does not move significantly from zero for frequencies below 20 Hz; the remaining part of the spectrum is well fit by the theoretical curve. The variance and skew of the filtered records can then be used to compute reliably mepp frequency and amplitude.

In two experiments, both in Ca^{2+}-free solution, the distortion of the spectrum gave a major contribution to the variance. They were therefore discarded. The power spectrum in Fig. 2*B* is from one of these experiments. Even in these two experiments the shape of the averaged mepps obtained before and during ouabain effect were still well described by the difference of two exponentials (Fig. 3). Therefore, it is unlikely that the extracomponents in the spectra are due to changes in mepp time course.

To test the validity of the filtering procedure in our experimental conditions, and to choose empirically the appropriate filter time constant (RC), we analyzed a portion of an experiment with different RCs. Fig. 4 shows the values obtained for mepp frequency and amplitude, during 7 min of massive release, using filters with four different time constants. Consistent results were obtained with 1- and 2-ms RC, and this indicates that both filters were adequate in removing low

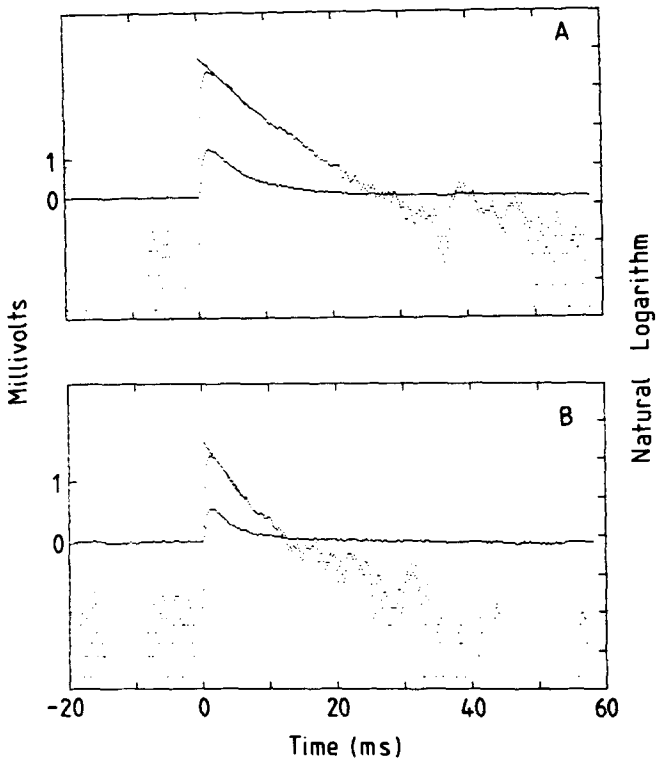

FIGURE 3 Waveforms of averaged mepps obtained at junctions treated with 0.05 mM ouabain. The waveforms are plotted both on linear and semilogarithmic scales. Ordinates: millivolts, left, and natural logarithm, right. Abscissae: time in milliseconds. On the semilogarithmic plot, the straight line obtained by linear regression fits the decay phase of the mepp well. The slope of this line yields the decay time constant of the mepp θ_1. The intercept at time = 0 is the amplitude factor, h; the rise time constant θ_2 is computed from θ_1 and the time to the peak. (*A*) 80 min after the application of ouabain in modified Ringer's solution. mepp frequency was <5/s; 20 events were averaged; the time constants were 6.11 and 0.64 ms; the amplitude factor, h, was 1.3 mV. (*B*) 78 min after addition of ouabain in Ca^{2+}-free solution. mepp frequency was 8/s; 25 events were averaged; the time constants were 4.25 and 0.38 ms; h was 0.52 mV. mepp waveforms in *A* and *B* were obtained from the same junctions used to prepare Fig. 2, *A* and *B*, respectively.

frequency contaminations. The time constant of 2 ms was used to analyze all experiments, because it gives a better signal/noise ratio.

Effects on mepp Parameters

Fig. 5 shows two typical examples of the effect of ouabain on mepp frequency. In the presence of Ca^{2+} mepp frequency increased exponentially to a peak, then dropped to lower values and gradually subsided (*C*). In Ca^{2+}-free solutions, on the other hand, the changes in mepp frequency were more gradual (*F*). These differences are also reflected in the time courses of cumulative quantal secretion. In the two experiments presented in Fig. 5, the h factor declined concomitantly with the increase in mepp frequency, and ultimately recovered to the initial values, whereas no relevant changes were observed in the two time constants of the mepp. However, consistent changes in h, θ_1, and θ_2 were not observed in all experiments.

The major results of all our experiments are summarized in Table I. Since the effects of 0.05 and 0.1 mM ouabain were not different, these results are combined. The peak frequency

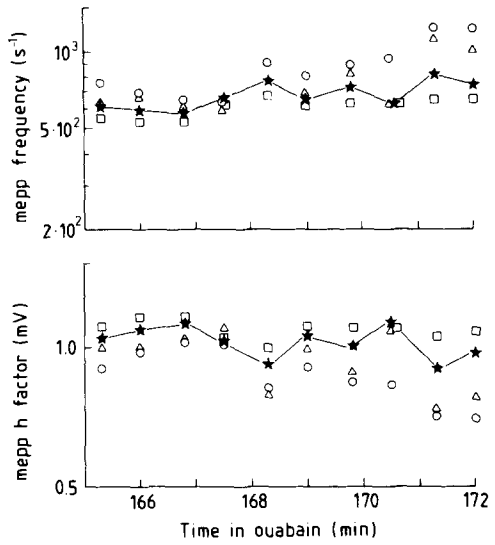

FIGURE 4 Estimates of mepp frequency and amplitude factor, h, at an actively secreting junction, using different filters. Abscissae: time after application of 0.1 mM ouabain in modified Ringer's solution (min). The continuous lines indicate the values obtained with the time constant (RC) used to analyze all experiments. O, RC = 11 ms; Δ, RC = 5 ms; ★, RC = 2 ms; □, RC = 1 ms. Notice the consistency of the values obtained with short RCs (1 and 2 ms).

TABLE I. *Effect of Ouabain on mepp Parameter*

	0.05-0.1 mM Ouabain 4 mM Mg^{2+} 1.8 mM Ca^{2+}*	0.05-0.1 mM Ouabain 0 Ca^{2+}, 4 mM Mg^{2+} 1 mM EGTA*
No. of junctions	6	5
Duration (min)‡	40 ± 12	56 ± 20
f-Peak × 10^{-3} (s^{-1})	1.3 ± 0.5	0.7 ± 0.4
Quanta secreted × 10^{-5}	7.4 ± 1.3§	8.8 ± 2.7§
V (mV) Control‖	86 ± 4	—
Initial	83 ± 4	73 ± 7
Peak	74 ± 6	60 ± 14
Final	78 ± 5	55 ± 13
ϑ_1 (ms) Control‖	6.5 ± 1.2	—
Initial	6.0 ± 0.6	4.5 ± 0.6
ϑ_2 (ms) Control‖	0.6 ± 0.2	—
Initial	0.6 ± 0.2	0.5 ± 0.2
h (mV) Control‖	1.0 ± 0.3	—
Initial	1.0 ± 0.2	0.7 ± 0.3
V_d Peak/initial¶	0.9 ± 0.05	0.8 ± 0.3
ϑ_1 Peak/initial	0.8 ± 0.2	1.0 ± 0.2
h Peak/initial	0.8 ± 0.2	0.8 ± 0.2

* No differences were found between 0.05 and 0.1 mM.
‡ Duration of the period of mepp frequency >10/s.
§ Not significantly different ($P > 0.1$, $t = 1.17$).
‖ Control values obtained only in four preparations.
¶ V_d, driving potential, the difference between membrane potential and equilibrium potential of ACh-gated endplate conductance channel, equated at −10 mV, a value in the middle of experimental measurements (26, 34).

in presence of Ca^{2+} was about twofold higher than in its absence; however, due to the faster decline of mepp frequency in the presence of Ca^{2+}, ~8 × 10^5 quanta were released under both conditions. The resting potential, V, recovered completely from the minimum values attained at the peak of mepp frequency in Ca^{2+}-containing solution, whereas it did not in Ca^{2+}-free solution. The prolonged impalement in the absence of Ca^{2+} may be responsible for the lack of complete

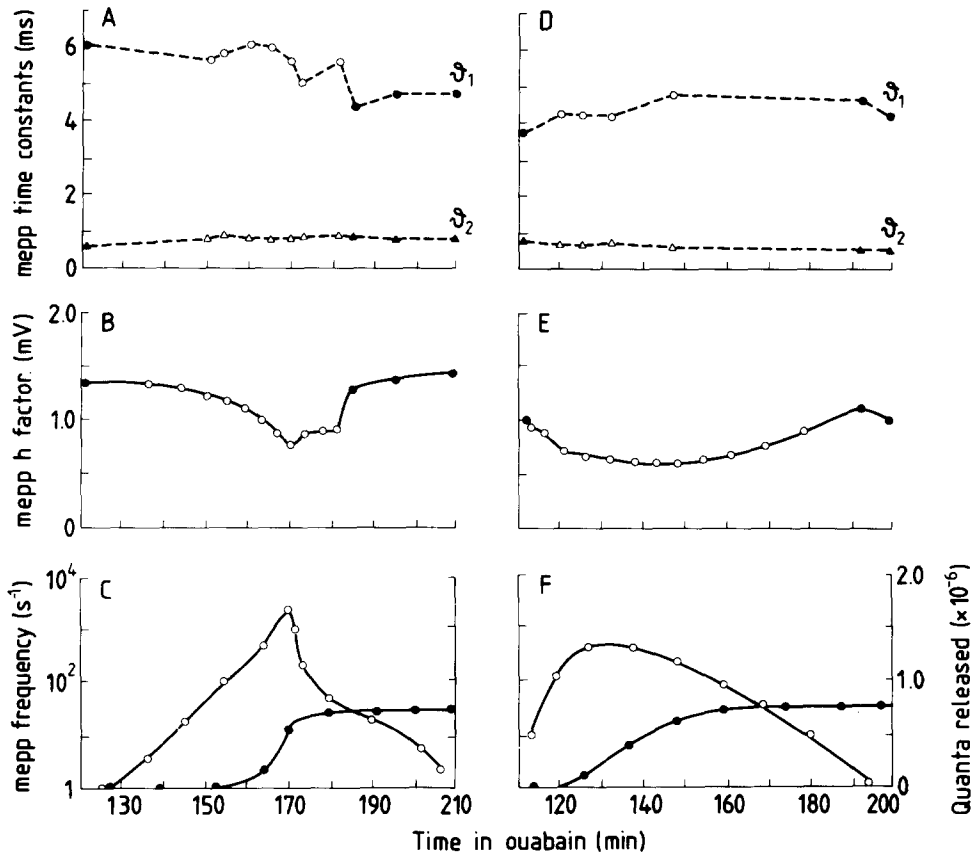

FIGURE 5 Time courses of the changes in mepp time constants, *h* factor, frequency, and number of quanta secreted at two junctions in 0.05 mM ouabain. (*A*, *B*, and *C*) Modified Ringer's solution. (*D*, *E*, and *F*) Ca^{2+}-free solution. Abscissae: time after addition of ouabain. In *A* and *D*, θ_1 is the decay time constant, and θ_2 is the rise time constant. The broken lines indicate that curves are obtained by joining measured values. Solid symbols are values obtained from averaged mepps, whereas open symbols are obtained from power spectra. The continuous lines in *B*, *C*, *E*, and *F* indicate that curves are obtained from consecutive estimates (one every 45 s). Open symbols are arbitrarily spaced, and solid symbols in *B* and *E* are values from averaged mepps; they coincide with the corresponding values from fluctuation analysis. Solid symbols in *C* and *F* indicate the number of quanta released, and open symbols indicate mepp frequency. The data shown in *A*, *B*, and *C* are from the same junction that was used to prepare Figs. 2 *A* and 3 *A*.

recovery. The mepp parameters remained unchanged during the lag period preceding the rise in mepp frequency, and the initial values given in Table I were obtained just before mepp frequency began to increase. The fractional reductions in driving potential, V_d, amplitude, *h*, and decay time constant, θ_1, indicate the changes occurring in these parameters at the peak frequency. The ratios are not significantly different from 1 in either conditions.

Morphology

Longitudinal sections and cross-sections from preparations fixed 60 min after the peak of quantal release induced by ouabain are shown in Figs. 6–10 and Figs. 14–16, respectively. A profound reduction in the number of synaptic vesicles is evident, independent of the presence of Ca^{2+}. Many deep invaginations of the prejunctional membrane originate from the region of axolemma between adjacent active zones. Occasionally these infoldings envelop Schwann cell processes, which are easily distinguishable because of their dense cytoplasm (Fig. 7). Under both conditions elaborate swirls of membrane are often found in the axoplasm. They are composed of two closely apposed layers of membrane, and frequently they form closed loops. Observations on serial sections clearly show that these structures are connected with the axolemma. The infoldings and the membrane loops often segregate, either partially or completely, clusters of synaptic vesicles from the prejunctional region of the axolemma (Figs. 8–10). The number of coated vesicles and coated pits is increased both in the presence and in the absence of extracellular Ca^{2+}. However this increase is more pronounced in Ca^{2+}-free solution (Figs. 8–10, and Table II). Coated vesicles are not randomly scattered within the terminal; they appear more concentrated in regions near the presynaptic membrane or in regions near the membrane material that appears in the axoplasm. Coated pits are seen budding either from membrane infoldings or directly from the axolemma at or between the active zones. The number of large vesicular structures is slightly increased in the terminals treated with ouabain both in the presence and in the absence of extracellular Ca^{2+}. The ultrastructure of mitochondria is frequently affected when Ca^{2+} is present in the medium. Swelling, disorganization of cristae, and clear matrix are the commonly encountered alterations of these organelles. The subcellular organization of muscle fiber and Schwann cell are not grossly modified by the prolonged exposure to ouabain.

The results of a complete morphometric analysis are sum-

FIGURES 6–8 Electron micrographs of longitudinal sections from three neuromuscular junctions. (Fig. 6) Resting preparation soaked for 3 h in modified Ringer's solution. (Fig. 7) 0.05 mM ouabain in modified Ringer's solution. (Fig. 8) 0.05 mM ouabain in Ca^{2+}-free solution. The terminals in Figs. 7 and 8 were fixed 60 min after the peak of mepp frequency. Notice the profound depletion of synaptic vesicles and the presence of extensive presynaptic membrane infoldings that penetrate deeply into the axoplasm. These infoldings arise from the prejunctional membrane (arrows) and frequently envelope projections of the Schwann cell (*P*). The infoldings partially segregate mitochondria (*m*) and clusters of synaptic vesicles (arrowheads). (Fig. 6) × 21,000; (Fig. 7) × 33,000; (Fig. 8) × 29,000.

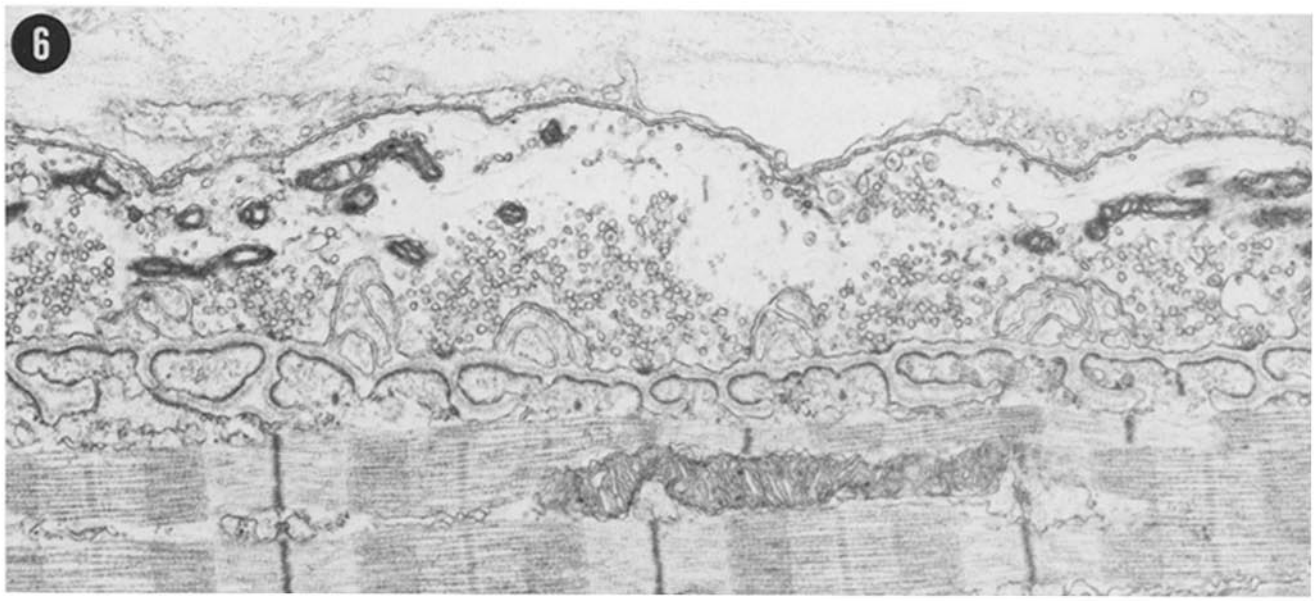
6


7
m
P

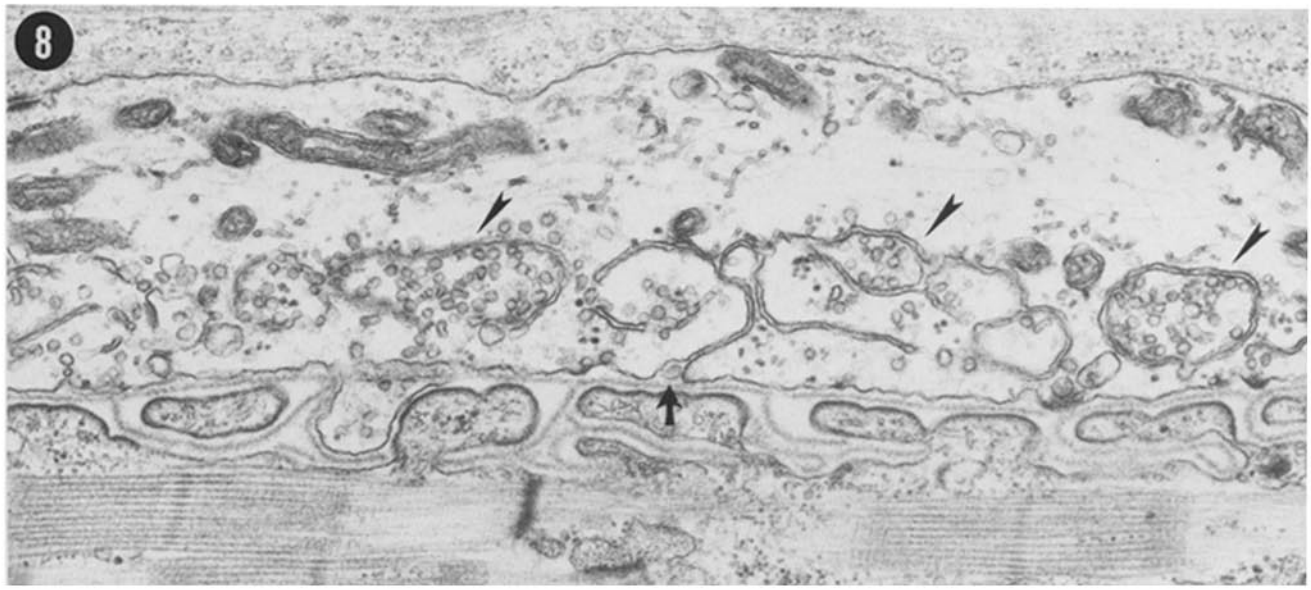
8

TABLE II. *Effect of Ouabain on Nerve Terminal Ultrastructure*

	Ringer's modified 4 mM Mg^{2+}	0.05–0.1 mM Ouabain 1.8 mM Ca^{2+}, 4 mM Mg^{2+} *	0.05–0.1 mM Ouabain 0 mM Ca^{2+}, 1 mM EGTA 4 mM Mg^{2+} *
Axolemma length ($\mu m/\mu m^2$)	1.9 ± 0.4	2.7 ± 0.5	2.4 ± 0.4
Infoldings of membrane ($\mu m/\mu m^2$)‡	0.5 ± 0.4	1.5 ± 0.9	1.6 ± 0.7
Synaptic vesicles (No./μm^2)	47 ± 18	13.7 ± 8.0	8.4 ± 5.0
Coated vesicles (No./μm^2)	0.4 ± 0.2	1.2 ± 0.5	2.3 ± 0.7
Large vesicular structures ($\mu m/\mu m^2$)§	0.3 ± 0.1	0.6 ± 0.3	0.4 ± 0.2
Total membrane length ($\mu m/\mu m^2$)‖	5.4	5.7	5.1
Axoplasm total area (μm^2)	146 (15)	125 (8)	101 (8)
Axoplasm cross-sectional area per terminal (μm^2)§	1.5 ± 0.5 (30)	1.7 ± 0.7 (30)	1.4 ± 0.5 (30)

All data are from muscles fixed 60 min after the peak of quantal release. All data except those in the last line were obtained from longitudinally sectioned neuromuscular junctions. Number of terminals are given in parentheses.

* No differences were found between 0.05 and 0.1 mM.

‡ The length of membrane is about twofold the length of the infoldings.

§ Except for the rows of data indicated by ‖ all values from ouabain-treated junctions are significantly different from control (*t*-tests, $P < 0.001$). The number of coated vesicles is significantly different between Ca^{2+}-containing and Ca^{2+}-free medium ($t = 6.07$, $P < 0.001$).

‖ This figure is the sum of the preceding values. The numbers of synaptic vesicles and coated vesicles were corrected as described at the end of the Results and transformed to membrane length, using values for diameters of 40 and 70 nm, respectively.

marized in Table II. Since there were no significant differences in the measured ultrastructural parameters between 0.05 and 0.1 mM ouabain, the data have been combined. After the exposure to ouabain there is a profound depletion (~75%) of synaptic vesicles both in the presence and in the absence of extracellular Ca^{2+}. The length of axolemma is slightly increased, and there is a great increase in total length of infoldings. The degree of depletion and the total length of the infoldings are not significantly different between the two experimental conditions.

Swelling of the terminal 60 min after the peak of release induced by ouabain was not evident by the inspection of individual micrographs from longitudinally sectioned neuromuscular junctions (Figs. 6–8). However changes in axoplasmic volume that cannot be correctly evaluated in longitudinal sections may yield erroneous estimates of the degree of synaptic vesicle depletion. We therefore completed the morphometric analysis with measurements of the areas of cross-sectioned terminals (Figs. 14–16). With the reasonable assumption that the total terminal length remained constant (see also reference 36), the results reported in Table II clearly indicate that axoplasmatic volume is not significantly changed 1 h after the peak of activity.

At the end of the 1 h of enhanced secretion, six preparations from experiments both with and without Ca^{2+} were extensively washed with fresh Ringer's solution for a total period of 2 h and then fixed. The terminals appear to be markedly swollen, they lack infoldings, and depletion of synaptic vesicles is virtually complete. Only a few synaptic vesicles, some coated vesicles, neurofilaments, elements of smooth endoplasmic reticulum, and swollen mitochondria are seen in the clear axoplasmatic field (Figs. 11 and 17). We measured the cross-sectional areas and lengths of the axolemma from preparations exposed to ouabain either in the presence (40 terminals) or in the absence (40 terminals) of extracellular Ca^{2+}. The cross-sectional area (3.3 ± 1.2 μm^2) is significantly increased with respect to control terminals and terminals fixed 1 h after the peak of activity (Table II). The cross-sectional length of axolemma (8.5 ± 2.3 μm) is also increased with respect to control (4.7 ± 0.7 μm).

The degree of depletion of synaptic vesicles at a nerve terminal during intense secretion of neurotransmitter depends on the balance between the rate at which vesicles are added to the axolemma and the rate at which they are removed from the axolemma (8). Depletion of synaptic vesicles and expansion of the axolemma are not observed at frog nerve terminals

FIGURE 9–13 Electron micrographs of longitudinal sections from five neuromuscular junctions, fixed during and after the peak of secretion induced by ouabain. (Figs. 9 and 10) Ouabain 0.05 mM in Ca^{2+}-free solution. The preparations were fixed 60 min after the peak of mepp frequency. Notice the elaborate swirls of membrane that segregate many synaptic vesicles and the presence of some coated vesicles. (Fig. 11) Ouabain 0.1 mM in modified Ringer's solution. 1 h after the peak of secretion the preparation was washed for 2 h in standard Ringer's solution without ouabain and then fixed. Notice the swelling of the terminal, the swelling of mitochondria, and the complete depletion of synaptic vesicles. (Figs. 12 and 13) Low power micrographs of portions of neuromuscular junctions exposed to ouabain 0.05 mM in the presence of HRP 1.5% and myoglobin 0.5%. (Fig. 12) Ouabain was added to modified Ringer's solution containing HRP, and the preparation was fixed 10 min after the onset of the high rate of secretion. The junctional cleft and the extracellular space between the Schwann cell (*Sc*) and the axolemma contain rich deposits of reaction product. The general organization of the axonal ending appears normal; however, many synaptic vesicles are clustered in regions near the presynaptic membrane. No synaptic vesicles containing reaction product are present in this field. A reduction in the number of vesicles in regions away from the prejunctional membrane and focal depletion of peripheral vesicles in areas along the prejunctional membrane are evident (asterisk). (Fig. 13 [unstained section]) Ouabain was added to Ca^{2+}-free solution containing HRP, and the preparation was fixed 30 min after the onset of the peak of secretion. The general distribution of reaction product is similar to that in Fig. 12. Elaborate infoldings of the axolemma are evident, and the spaces delimited by their membranes are marked by reaction product. (Fig. 9) × 35,000; (Fig. 10) × 35,000; (Fig. 11) × 28,000; (Fig. 12) × 16,500; (Fig. 13) × 16,000.

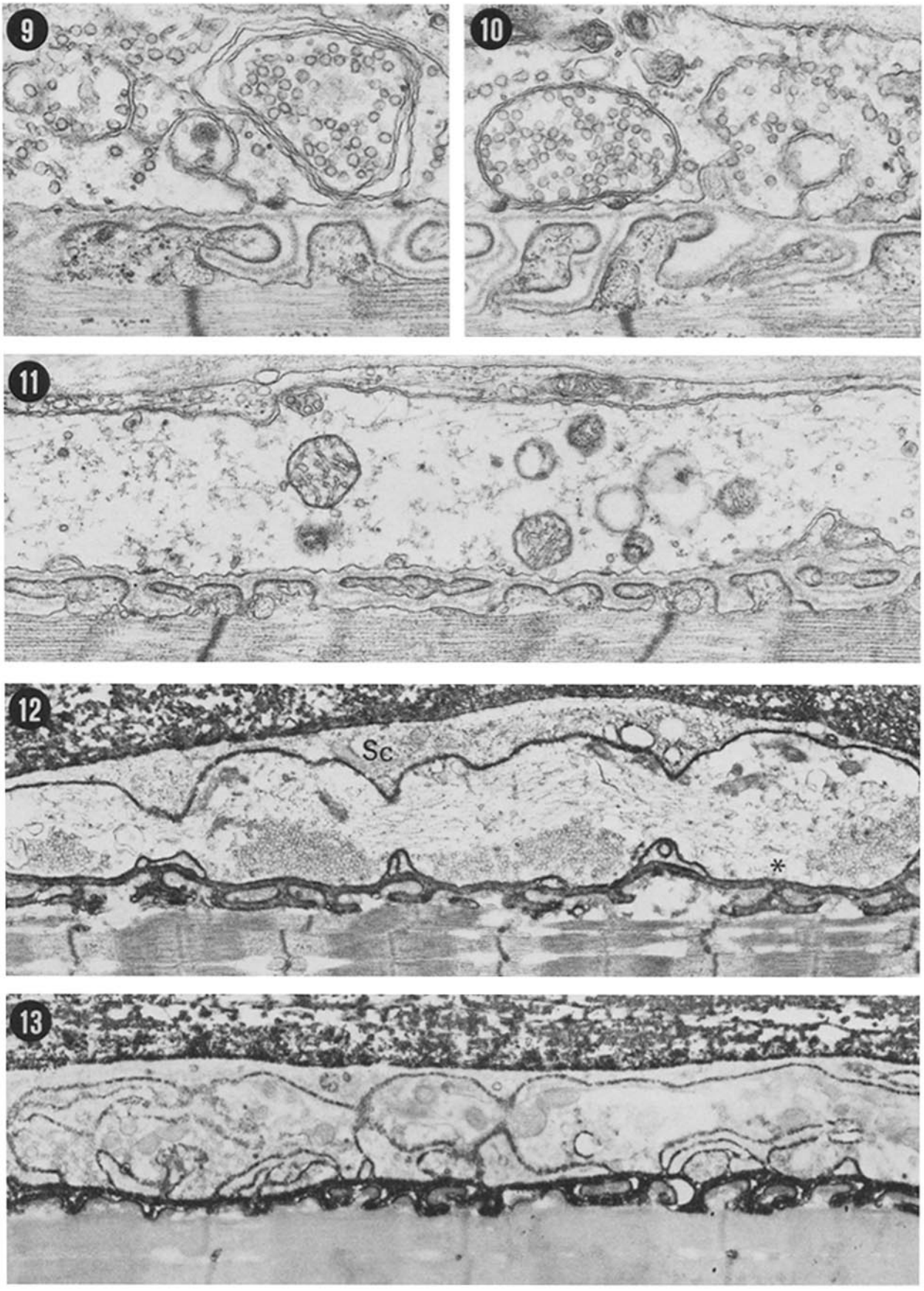
9
10
11
12
Sc
*
13

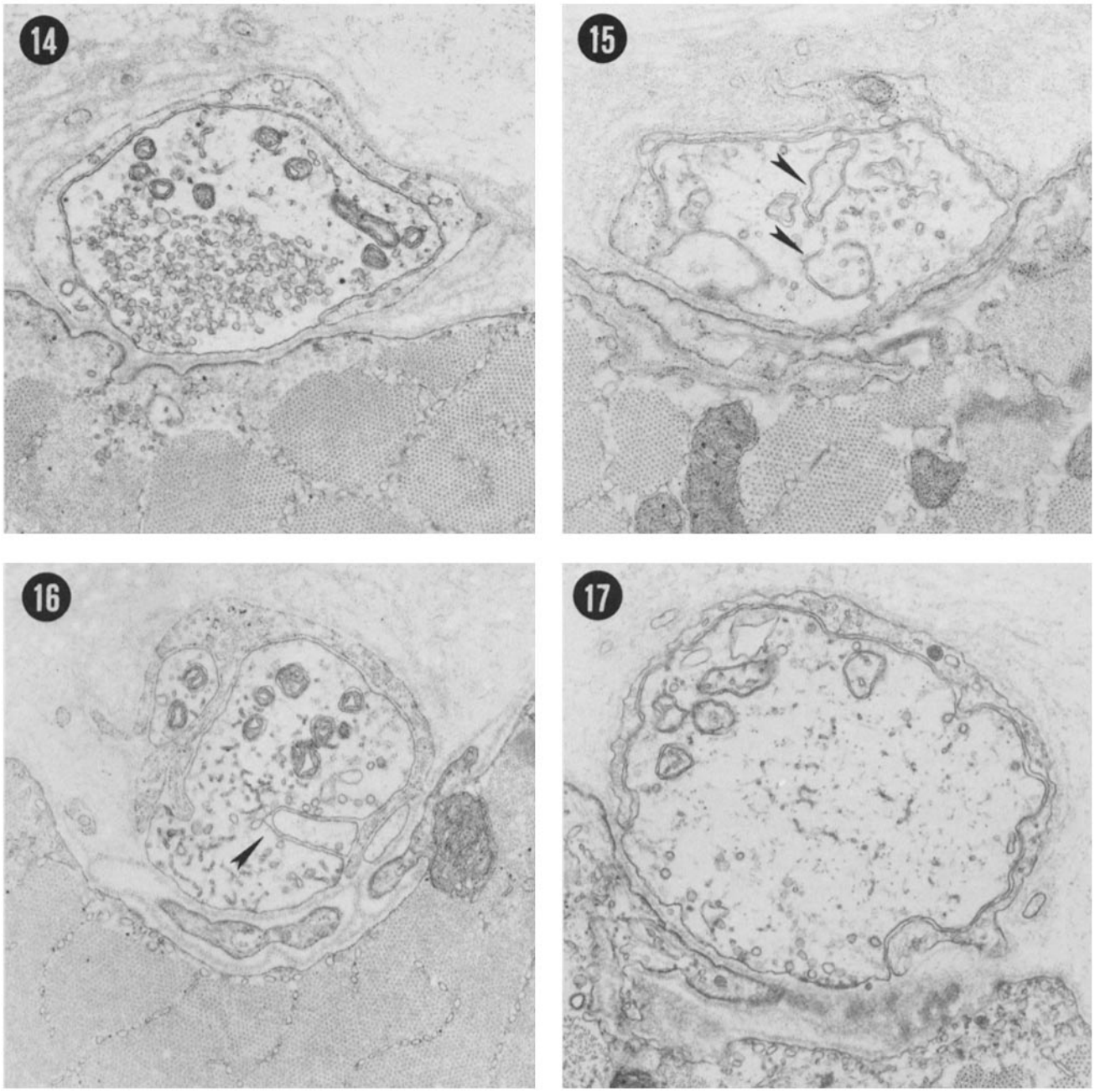

FIGURES 14–17 Electron micrographs of cross-sectioned frog neuromuscular junctions. (Fig. 14) Resting muscle soaked for 3 h in modified Ringer's solution. The cross-sectional area is 2.7 μm^2. (Fig. 15) Muscle fixed 60 min after the peak frequency induced by 0.1 mM ouabain applied in modified Ringer's solution. Notice the depletion of synaptic vesicles and the presence of some membrane infoldings (arrowheads). The cross-sectional area is 2.2 μm^2. (Fig. 16) Muscle fixed 60 min after the peak frequency induced by 0.1 mM ouabain applied in Ca^{2+}-free solution. Also in this case the depletion of synaptic vesicles and an infolding of the axolemma (arrowhead) are evident. The cross-sectional area is 2.0 μm^2. (Fig. 17) Preparation recovered for 2 h in standard Ringer's solution without ouabain, 60 min after the peak secretion induced by 0.1 mM ouabain in Ca^{2+}-free solution. The depletion of synaptic vesicles is almost complete and is accompanied by a profound swelling of the terminal. The cross-sectional area is 4.6 μm^2. × 25,000.

after several hours of stimulation at 2/s, and active vesicle recycling has been shown to operate under these conditions (7, 11, 12). A significant depletion of synaptic vesicles occurs at frog neuromuscular junction either when the rate of secretion of quanta exceeds several thousand per second (10, 33) or when the recovery limb of the vesicle cycle has been fatigued or impaired (9). The maximum rate of secretion induced by ouabain is $\sim 10^3$/s; thus, it seems that the rapid depletion observed is due only to the impairment of some factors in the axoplasm that determine the rate of recovery.

To test more directly this suggestion we carried out experiments in which HRP was present in the bathing solution. Fig. 12 is an example of a neuromuscular junction fixed 10 min after the mepp frequency had increased over 100/s, whereas Fig. 13 is an example of a junction fixed after 30 min of intense activity (i.e., after the peak). Electron-dense reaction

product fills the vast extracellular space between muscle fibers, the space delimited by the pre- and post-synaptic membranes, the junctional folds, and the secluded space between the Schwann cell processes and the axolemma. Reaction product is also present in the t-tubules of the muscle fibers. When preparations are fixed at an early stage of the secretion many synaptic vesicles are still present in the nerve terminals. They are clustered in regions of the axoplasm adjacent to the presynaptic membrane, and only a few are loaded with reaction product (Fig. 12). A reduction in the number of vesicles in regions away from the prejunctional membrane and focal depletion of peripheral vesicles along the prejunctional membrane are evident. However, extensive infoldings of the axolemma are not seen at this stage. On the other hand, when preparations are fixed later during the secretory period, the number of synaptic vesicles is substantially reduced, and many deep invaginations of the axolemma or elaborate loops of membrane develop. Reaction product is also found in the narrow spaces between membrane invaginations or loops, indicating that they originate from the nerve terminal axolemma. In this case as well, very few vesicles are loaded with reaction product (Fig. 13).

The mean thickness of the sections we used for electron microscopy is estimated to be ~40 nm (silver-gray color) (37). Therefore the apparent concentration of synaptic vesicles was ~1150 ± 450/μm^3 in resting terminals. This value is an overestimate of the real vesicle number since it includes profiles of vesicles whose centers are not included in the section. It should be reduced by $1 + d/L$, where d is the mean vesicle diameter (40 nm) and L is the mean section thickness. Thus, the real vesicle concentration is 575 ± 225/μm^3. This figure is ~60% of that reported by Birks et al. (5) for terminals in frog sartorius muscle. The average length of the total terminal arborization revealed by cholinesterase reaction in frog cutaneous pectoris muscle is ~600 ± 200 μm (25, 36), and the average cross-sectional area from resting terminals is 1.5 μm^2 (Table II). Thus, our estimate of the number of vesicles per resting terminal is of the order of 5×10^5.

DISCUSSION

The method of measuring mepp rates and amplitudes from the skew and variance at rapidly secreting neuromuscular junctions has been shown to yield valid results under conditions where the conventional method of noise analysis, based upon the mean and the variance, cannot be applied (33). These conditions include (*a*) the presence of sources of depolarization other than linear summation of mepps; (*b*) changes in membrane properties during the course of secretion (leading to the so-called nonlinear summation of mepps); (*c*) nonstationarity. Indeed, the increase in mepp frequency induced by ouabain is often nonstationary. Our results do not allow us to conclude that the extracomponents present in most power spectra are entirely due to nonstationarity in the rate of release. However, we analyzed only those experiments in which the extracomponents were small so that the spurious contributions were effectively removed by appropriate filtering (18, 19). Thus, we were able to measure reliably the total number of quanta secreted under these nonideal conditions, and to correlate these results with the morphometric measurements of the concurrent changes in nerve terminal ultrastructure.

We have thoroughly studied the effect of ouabain at frog neuromuscular junctions bathed either in modified Ringer's solutions containing Ca^{2+} or in Ca^{2+}-free solution. The time course of secretion was different in the two experimental conditions, and we cannot account for this difference. In spite of this, the integration over time of the rates of secretion indicates that the cumulative quantal releases were not significantly different: 7.4×10^5 quanta in Ca^{2+}-containing and 8.8×10^5 in Ca^{2+}-free solution.

When BWSV is applied to unstimulated terminals, it provokes an enormous increase in mepp frequency (23, 28) and almost completely depletes the terminals of their store of quanta and synaptic vesicles (13, 20). Therefore, the increase in mepp rates induced by BWSV active component, α-LTx, can be used as a measure of the store of transmitter existing in a terminal at the time of application (12). We applied α-LTx to two preparations at the end of the period of secretion induced by ouabain, and no significant increase in mepp frequency was observed. We therefore concluded that ouabain almost completely depletes nerve terminals of their quantal stores.

Previous estimates of the initial store of quanta at neuromuscular junctions of frog cutaneous pectoris muscle vary between 2.5×10^5 and 6×10^5 (7, 12). Hence, our electrophysiological results suggest that the initial store of quanta is secreted completely by ouabain, without relevant turnover.

If a quantum is secreted from synaptic vesicles by exocytosis, then our results imply that the resting population of synaptic vesicles should be entirely used during the period of secretion induced by ouabain, with little or no recycling of vesicle membrane.

Our morphometric analysis indicates that the total number of synaptic vesicles present in resting terminals is of the order of 5×10^5. This number is reduced by ~75% after the treatment with ouabain. Furthermore, the surface area of the axolemma expands to form extensive and elaborate infoldings that deeply penetrate into the axoplasm. This finding suggests that ouabain, like BWSV, interferes with the recycling process that normally operates in maintaining the vesicle population in the face of intense secretion of neurotransmitter (23). The lack of uptake of HRP during the effect of ouabain supports such an interpretation. It has been reported that ouabain enhances vesicular uptake of HRP in retinal photoreceptors, without formation of HRP-labeled cisternae in the first half hour (27). Our results suggest that the effect of ouabain on frog motor nerve endings is quite different. We cannot completely rule out the possibility that some vesicle recycling may have occurred at an early stage of the ouabain-induced secretion. However, the rapid depletion achieved indicates that, if present, it should be of a limited extent. It has been suggested that newly formed synaptic vesicles release preferentially quanta of ACh (38). If this were the case also in our experiments, then some vesicle recycling might have occurred without being detectable from HRP studies, performed when mepp frequency has risen over 100/s. Certainly if some recycling had occurred this would improve the correlation between our estimates of the number of quanta secreted and the resting store of vesicles. However, other factors may have contributed to the observed differences. Among them are: (*a*) our fluctuation analysis is reliable with 10% of error (see Material and Methods); (*b*) the correct estimate of the number of vesicles in our resting terminals hangs on the validity of some assumptions (e.g., the constancy of the section thickness,

the uniform distribution of synaptic vesicles within the entire volume of the nerve terminal). In spite of these uncertainties it appears that in ouabain the recycling of both ACh quanta and vesicle membrane are severely impaired, and there is good correlation between the total number of quanta secreted and the decline in number of synaptic vesicles. The membrane of synaptic vesicles remains permanently incorporated into the infoldings of the axolemma. Indeed 60 min after the peak secretion a good membrane balance can be drawn from the data presented in Table II in both experimental conditions. The omission of Ca^{2+} delays the development of the changes in secretion. However, it has no large effect either on the final morphological state of the terminals or on the cumulative quantal release.

The present results are different from those recently reported with La^{3+} using a similar procedure (33). The total number of quanta secreted at La^{3+}-treated junctions is several-fold greater than the initial store of vesicles. Thus, under the effect of La^{3+} the quantal store appears to turn over several times during the course of the prolonged secretion, and this multiple turnover is sustained by an active vesicle recycling. Depletion and extensive infoldings are observed only at the end; by then, it is likely that the very active secretion had severely taxed the capacity of the system responsible for the interiorization of vesicle membrane, so that the rate of vesicle formation from the axolemma was seriously slowed down (11).

Ouabain, on the other hand, seems to interfere early with the recycling process so that it causes a profound depletion of synaptic vesicles during the secretion of a number of quanta roughly equal to the number of vesicles present in resting terminals. From the data reported in Table I a number of quanta that lie in the range of $5–10 \times 10^5$ were secreted in our experiments. This figure is then an upper limit for the number of quanta stored in resting terminals. It is an upper limit because one cannot rule out the possibility that some turnover may have occurred during the early period of ouabain-induced secretion.

It is interesting that the extensive infoldings of the axolemma are not seen any more in terminals that have been washed for 2 h in Ringer's solution, even though the loss of vesicles from the terminals is more complete than immediately after the period of intense secretion. The terminals appear swollen and contain swollen mitochondria. These late changes in the ultrastructure may be simply due to the ionic unbalance that occurs within the terminal as the consequence of the prolonged inhibition of the Na^+ pump. Indeed, at the neuromuscular junction the inhibition of the Na^+ pump by the cardiac glycosides is very slowly reversible after removal of the drug from the bathing medium (4). When ouabain was removed, mepp frequency was ~5/s. If the same rate of secretion was maintained throughout the wash in Ringer's solution, the total quantal secretion during this period would have been ~40,000 quanta. This figure represents 8% of the initial store of vesicles, and could partially account for the loss of the residual vesicles observed in preparations fixed immediately after the period of secretion.

Whatever the cause, it appears that the swelling of the terminal is accompanied by an increase in the surface area of the axolemma. Assuming the nerve terminal branches are circular in cross-section, then from the present data the total surface area of a resting terminal may be estimated on the order of 2,500 μm^2 and the total surface area of a swollen terminal on the order of 5,000 μm^2. Our figure of the amount of synaptic vesicles present in resting terminals is $\sim 5 \times 10^5$, thus we estimated a ratio of ~1 for the area of synaptic vesicle membranes to the area of axolemma. This estimate predicts that the area of the axolemma would increase about twofold if all the vesicle membranes were incorporated into it. Therefore it appears that the extramembrane needed to surround the swollen terminals derives from vesicles that have been permanently incorporated into the axolemma.

Taken all together these findings support the vesicle hypothesis of the release of quanta of ACh, in the sense that there is a good correlation, in the absence of extensive vesicle recycling, between the reduction in the store of synaptic vesicles and the total number of quanta secreted.

Finally we observed an increase in the number of coated vesicles and coated pits. An increase in the number of coated vesicles has been previously reported at frog neuromuscular junctions, under conditions of active recycling of vesicle membrane, and the hypothesis was proposed that recycling of vesicle membrane requires several successive steps: concentration of specific vesicle components in selective regions of the axolemma, formation of coated vesicles that coalesce to form intraterminal cisternae, and budding of new synaptic vesicles from the cisternae (22). More recently it has been proposed that another nonselective endocytosis mechanism may operate at frog neuromuscular junctions through invagination at the active zone of large uncoated vacuoles (30). Vesicle recycling is severely impaired in our experiments, despite the increase in the number of coated vesicles. It is difficult to account for the increase we observed but it is possible that the burden of maintaining the vesicle population is normally sustained by quick, direct removal of small uncoated vesicle membrane (8, 12), and that the increase in the surface area of the axolemma may activate the endocytotic mechanism via coated vesicles, as previously suggested (29). However, we cannot exclude that during ouabain effect recovery of the vesicle specific proteins by coated vesicles is normal or even activated but the recovery of large vacuoles has failed. Finally, it has also been suggested that an increase in the number of coated pits may result, in nonneuronal cells, as direct consequence of the impairment of endocytosis through coated vesicles (24).

We are indebted to Dr. W. P. Hurlbut of The Rockefeller University who kindly allowed us to use the Digital Equipment Corp. PDP 11/23 plus computer and for helpful discussion and suggestions. We thank Dr. J. Meldolesi who kindly supplied the purified α-Latrotoxin, and Dr. L. Guglielmino, who helped in preliminary experiments. We gratefully acknowledge the assistance of A. Galli and N. Iezzi who helped with electron microscopy, P. Tinelli and F. Crippa who prepared the illustrations, and Mrs. S. Avogadro who typed the manuscript.

This work was partially supported by a grant from the Muscular Dystrophy Association of America, Inc. (to B. Ceccarelli). R. Fesce was supported by U. S. Public Health Service grant NS18354 (W. P. Hurlbut).

Received for publication 19 November 1984, and in revised form 22 July 1985.

REFERENCES

1. Baker, P. F., and A. C. Crawford. 1975. A note on the mechanism by which inhibitors of the sodium pump accelerate spontaneous release of transmitter from motor nerve terminals. *J. Physiol. (Lond.).* 247:209–226.

2. Bendat, J. S., and A. G. Piersol. 1971. Random Data: Analysis and Measurement. John Wiley & Sons, Inc., New York. 407 pp.
3. Birks, R. I. 1962. The effect of a cardiac glycoside on subcellular structures within nerve cells and their processes in sympathetic ganglia and skeletal muscle. *Can. J. Biochem. Physiol.* 40:303–315.
4. Birks, R. I., and M. W. Cohen. 1968. The action of sodium pump inhibitors on neuromuscular transmission. *Proc. R. Soc. Lond. B Biol. Sci.* 170:381–399.
5. Birks, R., H. E. Huxley, and B. Katz. 1960. The fine structure of the neuromuscular junction of the frog. *J. Physiol. (Lond.).* 150:134–144.
6. Campbell, N. 1909. Discontinuous phenomena. *Proc. Cambridge Phil. Soc.* 15: 117–136.
7. Ceccarelli, B., and W. P. Hurlbut. 1975. The effects of prolonged repetitive stimulation in hemicholinum on the frog neuromuscular junction. *J. Physiol. (Lond.).* 247:163–188.
8. Ceccarelli, B., and W. P. Hurlbut. 1980. Vesicle hypothesis of the release of quanta of acetylcholine. *Physiol. Rev.* 60:396–441.
9. Ceccarelli, B., and W. P. Hurlbut. 1981. Ca^{2+}-dependent recycling of synaptic vesicles at the frog neuromuscular junction. *J. Cell Biol.* 87:297–303.
10. Ceccarelli, B., F. Grohovaz, and W. P. Hurlbut. 1979. Freeze-fracture studies of frog neuromuscular junctions during intense release of neurotransmitter. II. Effects of electrical stimulation and high potassium. *J. Cell Biol.* 81:178–192.
11. Ceccarelli, B., W. P. Hurlbut, and A. Mauro. 1972. Depletion of vesicles from frog neuromuscular junctions by prolonged tetanic stimulation. *J. Cell Biol.* 54:30–38.
12. Ceccarelli, B., W. P. Hurlbut, and A. Mauro. 1973. Turnover of transmitter and synaptic vesicles at the frog neuromuscular junction. *J. Cell Biol.* 57:499–524.
13. Clark, A. W., W. P. Hurlbut, and A. Mauro. 1972. Changes in the fine structure of the neuromuscular junction of the frog caused by black widow spider venom. *J. Cell Biol.* 52:1–14.
14. Cornog, J. L., N. K. Gonatas, and J. R. Feierman. 1967. Effects of intracerebral injection of ouabain on the fine structure of rat cerebral cortex. *Am. J. Pathol.* 51:573–581.
15. Del Castillo, J., and B. Katz. 1956. Biophysical aspects of neuro-muscular transmission. *Prog. Biophys. Biophys. Chem.* 6:121–170.
16. Del Castillo, J., and B. Katz. 1957. La base "quantale" de la transmission neuromusculaire. *Colloq. Int. Cent. Natl. Rech. Sci.* 67:245–258.
17. Elmiqvist, D., and D. S. Feldman. 1965. Effects of sodium pump inhibitors on spontaneous acetylcholine release at the neuromuscular junction. *J. Physiol. (Lond.).* 181:498–505.
18. Fesce, R. 1985. Fluctuation analysis applied to non-stationary biological processes. *In* Calcium, Neuronal Function and Transmitter Release. B. Katz and R. Rahamimoff, editors. Martinus Nijhoff/Dr. W. Junk Publishers, Jerusalem. In press.
19. Fesce, R., J. R. Segal, B. Ceccarelli, and W. P. Hurlbut. 1985. Measurements of the rate of quantal secretion induced by black widow spider venom (BWSV) at the endplate. *Biophys. J.* 47:477a. (Abstr.)
20. Frontali, N., B. Ceccarelli, A. Gorio, A. Mauro, P. Siekevitz, M.-C. Tzeng, and W. P. Hurlbut. 1976. Purification from black widow spider venom of a protein factor causing the depletion of synaptic vesicles at neuromuscular junctions. *J. Cell Biol.* 68:462–479.
21. Graham, R. C., and M. J. Karnowsky. 1966. The early stages of absorption of injected horseradish peroxidase in the proximal tubule of the mouse kidney; ultrastructural cytochemistry by a new technique. *J. Histochem. Cytochem.* 14:291–302.
22. Heuser, J. E., and T. S. Reese. 1973. Evidence for recycling of synaptic vesicle membrane during transmitter release at the frog neuromuscular junction. *J. Cell Biol.* 57:315–344.
23. Hurlbut, W. P., and B. Ceccarelli. 1979. Use of black widow spider venom to study the release of neurotransmitter. *In* Advances in Cytopharmacology. Volume 3. B. Ceccarelli and F. Clementi, editors. Raven Press, New York. 87–115.
24. Kosaka, T., and K. Ikeda. 1983. Reversible blockage of membrane retrieval and endocytosis in the Garland cell of the temperature-sensitive mutant of *Drosophila melanogaster*, shibire^{ts1}. *J. Cell Biol.* 97:499–507.
25. Letinsky, M. S., K. H. Fischbeck, and U. J. McMahan. 1976. Precision of reinnervation of original postsynaptic sites in frog muscle after a nerve crush. *J. Neurocytol.* 5: 691–718.
26. Lewis, C. A. 1979. Ion concentraton dependence of the reversal potential and the single channel conductance of ion channels at the frog neuromuscular junction. *J. Physiol. (Lond.).* 286:417–445.
27. Liscum, L., P. J. Hauptman, D. C. Hood, and E. Holtzman. 1982. Effect of barium and tetraethylammonium on membrane circulation in frog retinal photoreceptors. *J. Cell Biol.* 95:296–309.
28. Longenecker, H. E., W. P. Hurlbut, A. Mauro, and A. W. Clark. 1970. Effects of black widow spider venom on the frog neuromuscular junction. *Nature (Lond.).* 225:701–705.
29. Meldolesi, J., and B. Ceccarelli. 1981. Exocytosis and membrane recycling. *Philos. Trans. R. Soc. Lond. B Biol. Soc.* 296:55–65.
30. Miller, T. M., and J. E. Heuser. 1984. Endocytosis of synaptic vesicle membrane at the frog neuromuscular junction. *J. Cell Biol.* 98:685–698.
31. Rice, S. O. 1944. Mathematical analysis of random noise. *Bell Syst. Tech. J.* 23:282–332.
32. Schick, K. L. 1974. Power spectra of pulse sequences and implications for membrane fluctuations. *Acta Biotheor.* 23:1–17.
33. Segal, J. R., B. Ceccarelli, R. Fesce, and W. P. Hurlbut. 1985. Miniature endplate potential frequency and amplitude determined by an extension of Campbell's theorem. *Biophys. J.* 47:183–202.
34. Takeuchi, A., and N. Takeuchi. 1979. Active phase of frog's endplate potential. *J. Neurophysiol.* 22:395–411.
35. Tauc, L. 1982. Nonvesicular release of neurotransmitter. *Physiol. Rev.* 62:857–893.
36. Valtorta, F., L. Madeddu, J. Meldolesi, and B. Ceccarelli. 1984. Specific localization of the α-latrotoxin receptor in the nerve terminal plasma membrane. *J. Cell Biol.* 99:124–132.
37. Weibel, E. R., and D. Paumgartner. 1978. Integrated stereological and biochemical studies on hepatocytic membranes. II. Correlation of section thickness effect on volume and surface density estimates. *J. Cell Biol.* 77:584–597.
38. Zimmerman, H. 1979. Vesicle recycling and transmitter release. *Neurosci.* 4:1773–1804.